AIP Journal of Applied Physics

Electromigration in Pb-free Sn Ag 3.8 Cu 0.7 solder stripes

Ying-Chao Hsu, Chung-Kwuang Chou, P. C. Liu, Chih Chen, D. J. Yao, T. Chou, and K. N. Tu

Citation: Journal of Applied Physics **98**, 033523 (2005); doi: 10.1063/1.1999836
View online: http://dx.doi.org/10.1063/1.1999836
View Table of Contents: http://scitation.aip.org/content/aip/journal/jap/98/3?ver=pdfcov
Published by the AIP Publishing

Articles you may be interested in

Electromigration and critical product in eutectic SnPb solder lines at 100 ° C
J. Appl. Phys. **100**, 024909 (2006); 10.1063/1.2216487

Ternary bulk metallic glasses formed by minor alloying of Cu 8 Zr 5 icosahedron
Appl. Phys. Lett. **88**, 101907 (2006); 10.1063/1.2183367

Current crowding-induced electromigration in Sn Ag 3.0 Cu 0.5 microbumps
Appl. Phys. Lett. **88**, 072102 (2006); 10.1063/1.2173710

Electromigration failure mechanisms for SnAg 3.5 solder bumps on Ti Cr - Cu Cu and Ni (P) Au metallization pads
J. Appl. Phys. **96**, 4518 (2004); 10.1063/1.1788837

Electromigration of eutectic SnPb and SnAg 3.8 Cu 0.7 flip chip solder bumps and under-bump metallization
J. Appl. Phys. **90**, 4502 (2001); 10.1063/1.1400096

Re-register for Table of Content Alerts

Create a profile.

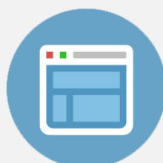

Sign up today!

[This article is copyrighted as indicated in the article. Reuse of AIP content is subject to the terms at: http://scitation.aip.org/termsconditions. Downloaded to] IP: 140.113.38.11 On: Thu, 01 May 2014 02:55:08

HTML ABSTRACT + LINKS

Electromigration in Pb-free $SnAg_{3.8}Cu_{0.7}$ solder stripes

Ying-Chao Hsu, Chung-Kwuang Chou, P. C. Liu, and Chih Chen[a)]
Department of Materials Science and Engineering, Chiao Tung University, Hsinchu, Taiwan 300, Republic of China

D. J. Yao
National Tsing Hua University, Institute of Microelectromechanical System, Hsinchu, Taiwan 300, Republic of China

T. Chou
Macronix International Corporation, Ltd., Hsinchu, Taiwan 300, Republic of China

K. N. Tu
Department of Materials Science and Engineering, University of California at Los Angeles (UCLA), Los Angeles, California 90095

(Received 22 February 2005; accepted 16 June 2005; published online 9 August 2005)

Electromigration behavior in the eutectic $SnAg_{3.8}Cu_{0.7}$ solder stripes was investigated in the vicinity of the device operation temperature of 100 °C by using the edge displacement technique. Measurements were made for relevant parameters for electromigration of the solder, such as drift velocity, threshold current density, activation energy, as well as the product of diffusivity and effective charge number (DZ^*). The threshold current densities were estimated to be 4.3×10^4 A/cm^2 at 80 °C, 3.2×10^4 A/cm^2 at 100 °C, and 1.4×10^4 A/cm^2 at 120 °C. These values represent the maximum current densities that the $SnAg_{3.8}Cu_{0.7}$ solder can carry without electromigration damage at the three stressing temperatures. The electromigration activation energy was determined to be 0.45 eV in the temperature range of 80–120 °C. The measured products of diffusivity and the effective charge number, DZ^*, were -1.8×10^{-10} cm^2/s at 80 °C, -5.0×10^{-10} cm^2/s at 100 °C, and -7.2×10^{-10} cm^2/s at 120 °C. *© 2005 American Institute of Physics*. [DOI: 10.1063/1.1999836]

I. INTRODUCTION

Flip-chip technology is widely used in advanced electronic products because of its higher packaging density, better performance, smaller device footprints, and lower packaging profiles.[1] The design rule of packaging requires that each flip-chip solder bump will carry 0.2–0.4 A, and the size of these solder bumps is already quite small, with a diameter of about 100 μm or less. The average current density in a bump approaches 10^4 A/cm^2. To meet the future performance requirements, even in handheld consumer products, the applied current density will increase. With the trend of miniaturization, electromigration in solder joints has been recognized as an important reliability issue for flip-chip technology.[2,3]

With increasing environmental concerns, the application of Pb-free solders to consumer electronic products has become a market driving force.[4,5] The Congress of the European Union has a directive to ban the use of Pb-based solder on July 1, 2006. Among the Pb-free solders, eutectic $SnAg_{3.8}Cu_{0.7}$ solder appears to be the most promising candidate for replacing the eutectic SnPb solder. Indeed, the National Electronics Manufacturing Initiative (NEMI) has recommended replacing the eutectic SnPb alloy with the eutectic SnAgCu alloy in reflow processing.[6] In the initial period of mass production of Pb-free components, reliability issues such as electromigration in the SnAgCu solder are of urgent concern.

Several studies have addressed the electromigration issue of SnAgCu alloy.[7–12] Choi *et al.* measured the mean time to failure (MTTF) of eutectic SnAgCu bumps, and they attempted to determine the effective charge number (Z^*) of the solder by marker movement.[7] But the marker movement was too small to be measured. Lin *et al.* investigated the current carrying capability of eutectic SnAgCu bumps, and found that there was no electromigration damage in the bumps after stressing by 2.5×10^4 A/cm^2 at 150 °C for 2338 h.[12] However, the relevant parameters of electromigration, such as threshold current density (J_c), drift velocity, activation energy (E_a), and the product of diffusivity and the effective charge number (DZ^*) of the eutectic SnAgCu solder are still unknown.

This lack of information is because of the difficulty in preparing Blech-type electromigration test specimens of SnAgCu solder. Blech developed a unique set of test structures of short stripes of Al on a TiN base line for the measurement of the drift velocity of electromigration so that the relevant parameters of electromigration can be determined.[13,14] However, eutectic SnAgCu solder stripes have not been deposited by evaporation, sputtering, or electroplating. In addition, the solder is very soft, and it is hard to pattern it into short stripes. In this study, we report a process to fabricate solders Blech specimens, and we employed

[a)]Author to whom correspondence should be addressed; electronic mail: chih@cc.nctu.edu.tw

[This article is copyrighted as indicated in the article. Reuse of AIP content is subject to the terms at: http://scitation.aip.org/termsconditions. Downloaded to] IP: 140.113.38.11 On: Thu, 01 May 2014 02:55:08

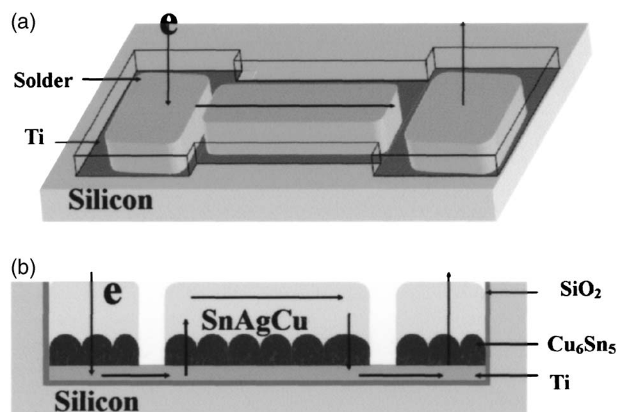

FIG. 1. (a) Tilted-view schematic of the solder stripe on a Ti film in a Si trench. (b) Cross-sectional schematic of the solder Blech specimen. The direction of the electron flow is indicated by the arrows.

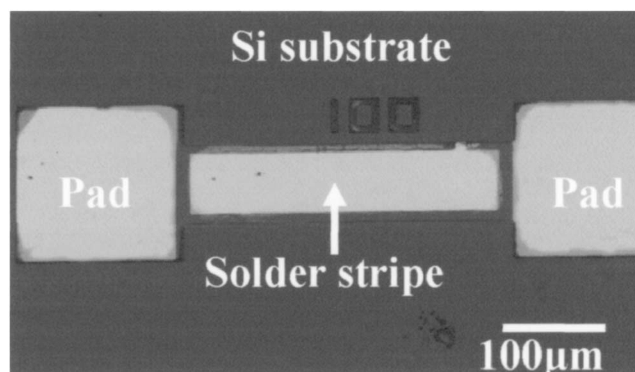

FIG. 2. BSE SEM image of the fabricated dumbbell-shaped stripe.

atomic force microscopy (AFM) to measure the depletion volume and drift velocity on the cathode side. As a result, we obtained a direct and precise measurement of the solder electromigration parameters.

II. EXPERIMENT

A similar process to fabricate Blech's specimens of Al stripe is adopted to fabricate the solder specimens. The main difference here is that the solder Blech specimen was fabricated in a Si trench, in which the top Si surface served as a polishing stopper during the subsequent polishing process. A 4-in. *p*-type Si wafer was cleaned by piranha solution (H_2O_2 and H_2SO_4 at the ratio of 1:7) for 10 min at 100 °C. After cleaning, the silicon wafer was patterned by photolithography and deep reactive ion etching (DRIE) to form dumbbell-shaped trenches of 3.1 μm in depth. Then, a 1200-Å SiO_2 insulating layer was grown on the wafer. Subsequently, titanium and copper films with thicknesses of 1700 and 4000 Å, respectively, were thermally evaporated onto the silicon wafer by an e-beam evaporator. Thereafter, the copper film inside the trench was patterned and selectively etched to form a short stripe, and two pads were also patterned on the Ti film, which served as a wetting metallization layer for the SnAgCu solder during the subsequent reflow process. Then the wafer was cut into small pieces, with a die in each piece. Solder paste of $SnAg_{3.8}Cu_{0.7}$ was applied to the Cu stripe at 230 °C for 2 s, in which the subscripts in $SnAg_{3.8}Cu_{0.7}$ stand for wt %. After the reflow process, the thickness of the solder may be over 10 μm thick, and its shape was bumplike. Therefore, a polishing procedure was needed to thin down the solder stripe. The thickness of the solder stripe was controlled by the thickness of the Si trench, since the top Si surface served as a polishing stop for the solder stripe.

Figures 1(a) and 1(b) illustrate the schematic diagrams of the tilted and cross-sectional views of the specimen, respectively. The two square pads at the two sides of the specimen were the electrodes, and the central solder stripe was the specimen to be studied. The stripe was 350 μm long and 80 μm wide. A layer of Cu_6Sn_5 intermetallic compound (IMC) grew between the Cu and the solder during the reflow, as shown in Fig. 1(b). The thickness of the solder was about 1–2 μm, and it varied from sample to sample due to the polishing process, which polished some of the Si stopper. The samples were then stressed at various current densities and temperatures, and the direction of the electron flow is indicated by the arrows in Figs. 1(a) and 1(b).

Transmission electron microscopy (TEM) and scanning electron microscopy (SEM) were employed to observe the microstructure of the solder stripes. Focused ion beam (FIB) was utilized to prepare cross-sectional TEM specimens. AFM was used to measure the depletion volume on the cathode side of the samples. Each specimen was scanned in AFM six times in order to measure the volume before and after the current stressing; the standard deviation was less than 1% compared with the average volume. The temperature increment due to the Joule heating effect was monitored by an infrared microscope, which has 0.1 °C temperature resolution and 2-μm spatial resolution.

III. RESULTS

A. Microstructure of the SnAgCu stripe and temperature measurement

Figure 2 demonstrates the backscattered electron (BSE) SEM image of the fabricated solder stripe, formed inside the Si trench. Typically, the four corners of the Cu stripe could not be wetted by molten solder paste during sample preparation. Figure 3(a) illustrates the cross-sectional TEM image of the specimen. A layer of scalloped Cu_6Sn_5 IMC is formed between the $SnAg_{3.8}Cu_{0.7}$ solder and the Cu layer. The SiO_2 and Ti layers can be clearly seen in the figure. The Cu film was consumed almost completely, but a few small Cu islands may be observed under some large IMCs. Since the Cu layer is not continuous, it is not considered when calculating the effective current density in the solder stripe. Figure 3(b) displays the enlarged cross-sectional TEM image of the area within the white circle in Fig. 3(a). The grain size was about 1 μm in diameter. We speculate that the minuscule grain size was due to the film thickness and the rapid cooling rate in the sample preparation process. Through theoretical calculations, it was found that about 80% of the applied current would flow inside the solder, whereas about 19% of the current drifted along the IMC layer, and only about 1% stayed in the Ti layer.

Figure 4 displays the measured temperature increment in the solder stripe as a function of current density at 80, 100,

[This article is copyrighted as indicated in the article. Reuse of AIP content is subject to the terms at: http://scitation.aip.org/termsconditions. Downloaded to] IP: 140.113.38.11 On: Thu, 01 May 2014 02:55:08

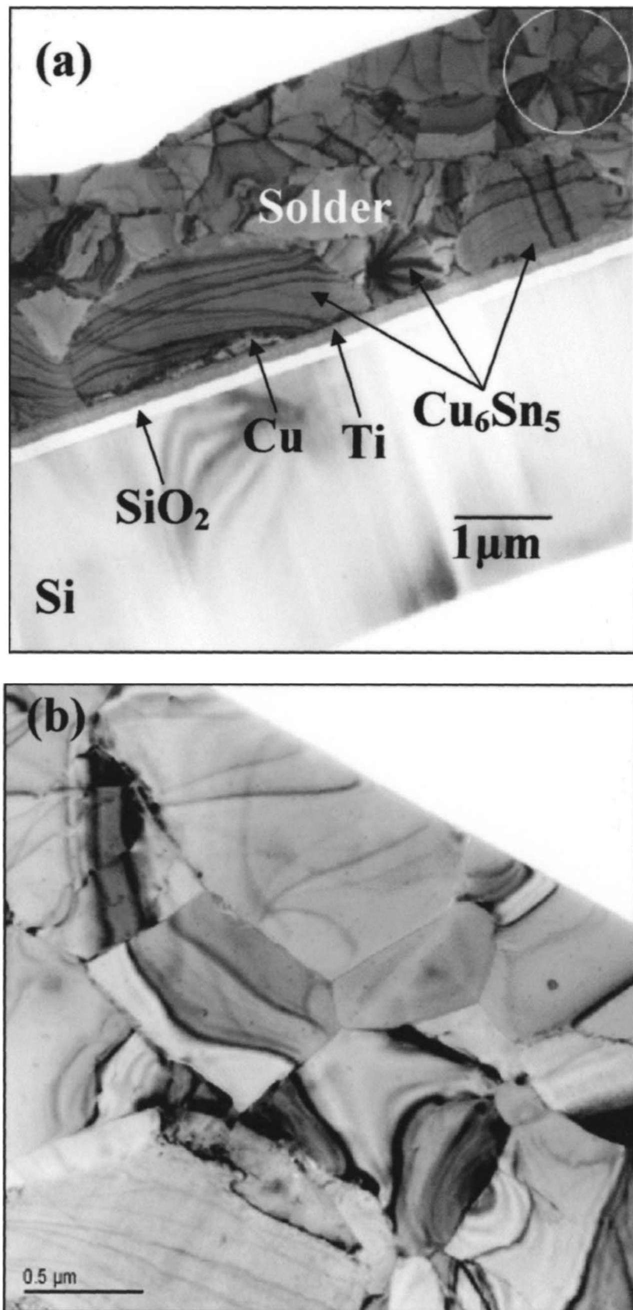

FIG. 3. (a) Cross-sectional TEM image of the solder Blech specimen. (b) Enlarged image of the white rectangular district in (a), with an average grain size of about 1 μm.

and 120 °C. The highest temperature increment was merely 5 °C when the specimen was stressed by 0.12 A, which corresponded approximately to 1×10^5 A/cm^2 in the solder stripes. The Joule heating effect in the stripes was much lower than that in the flip-chip solder bump.[15] This effect may be attributed to the stripe geometry and the excellent heat conduction of silicon substrate.

B. Threshold current density of the $SnAg_{3.8}Cu_{0.7}$ solder

Figures 5(a) and 5(b) show the SEM images of the $SnAg_{3.8}Cu_{0.7}$ solder stripe in the cathode end before and after the current stressing by 8.67×10^4 A/cm^2 at 80 °C for 65 h,

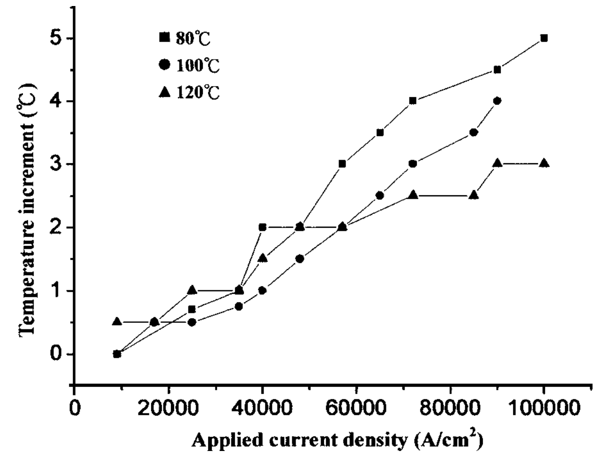

FIG. 4. Measured temperature increment inside the solder stripe as a function of applied current for the three stressing temperatures.

respectively. After the current stressing, the $SnAg_{3.8}Cu_{0.7}$ solder near the cathode was depleted by the electron flow, and the intermetallic compound at the cathode side was exposed, as shown in Fig. 5(b). Figures 5(c) and 5(d) show the corresponding three-dimensional (3D) AFM images for the solder stripes in Figs. 5(a) and 5(b), respectively. The AFM image in Fig. 5(d) also shows the depletion of the cathode end, which demonstrates that the AFM could measure the depletion of the solder. The depletion volume for this specimen was estimated to be 799 μm^3. On the other hand, hillocks were formed at the anode end of the stripe, as shown in Fig. 6. The composition of hillock is mainly Sn.

The average drift velocity of the solder stripe can be obtained by dividing the depletion volume (ΔV) by the product of the average cross-sectional area and the stressing time. Figure 7 displays the average drift velocity as a function of applied current density, showing a linear relationship for the three temperatures. By extrapolating the fitting line to the zero drift velocity, the threshold current density can be obtained. The estimated values are 4.3×10^4 A/cm^2 at 80 °C,

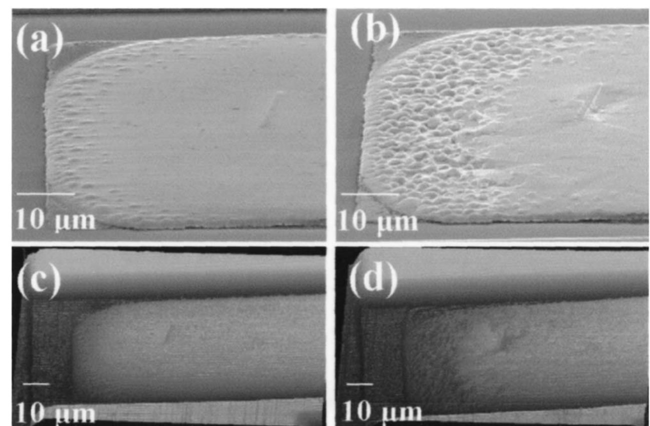

FIG. 5. (a) Tilted SEM image at the cathode side before current stressing. (b) Tilted SEM image on the cathode side after current stressing by 8.67 $\times10^4$ A/cm^2 at 80 °C for 65 h. The $SnAg_{3.8}Cu_{0.7}$ solder was migrated by the electron flow, but the IMC remained intact. (c) Corresponding AFM image of (a). (d) Corresponding AFM image of (b).

[This article is copyrighted as indicated in the article. Reuse of AIP content is subject to the terms at: http://scitation.aip.org/termsconditions. Downloaded to] IP: 140.113.38.11 On: Thu, 01 May 2014 02:55:08

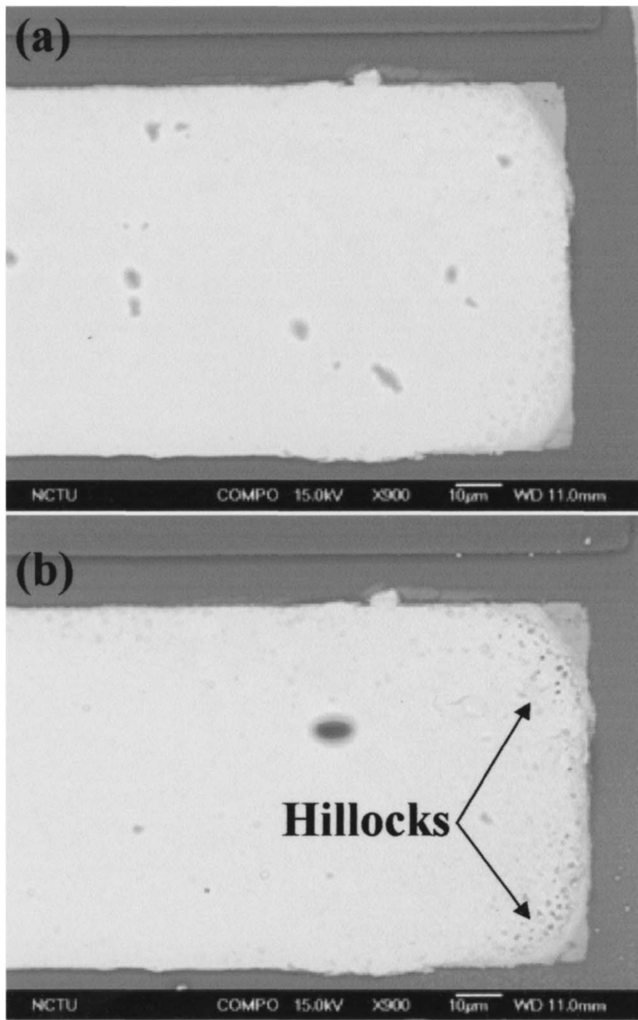

FIG. 6. Plan-view BSE SEM image of the anode side (a) before the current stressing, and (b) after the current stressing at 80 °C for 65 h. Hillocks are composed of almost pure Sn formed at the anode side.

3.2×10^4 A/cm^2 at 100 °C, and 1.4×10^4 A/cm^2 at 120 °C. These values represent the maximum current densities that the $SnAg_{3.8}Cu_{0.7}$ solder can carry without electromigration damage at the three stressing temperatures.

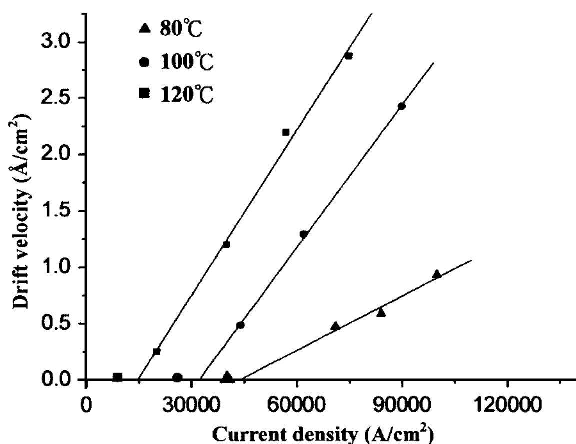

FIG. 7. Average drift velocity of the solder stripe as a function of applied current density. The threshold current densities were obtained by extrapolating the fitted lines to zero drift velocity.

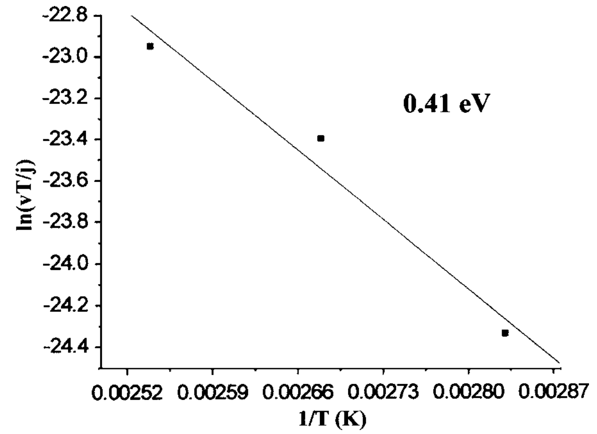

FIG. 8. Plot of the $\ln vT/j$ as a function of reciprocal temperature. The activation energy of 0.41 eV was obtained from the slope of the fitted line.

C. Activation energy and effective charge number of $SnAg_{3.8}Cu_{0.7}$ solder

The average drift velocity due to electromigration, as given by Huntigton and Grone,[16] is

$$\nu=\frac{J}{C}=BeZ^{*}\rho j=\left(\frac{D_0}{kT}\right)eZ^{*}\rho j\,\exp\left(\frac{-Ea}{kT}\right), \quad (1)$$

where J is the atom flux, C is the density of metal ions, B is the mobility, k is Boltzmann's constant, T is the absolute temperature, eZ^* is the effective charge of the ions, ρ is the metal resistivity, j is the electrical current density, E_a is the activation energy of diffusion, and D_0 is the prefactor of diffusion constant.

Equation (1) can be rewritten as

$$\frac{vT}{j}=\frac{D_0eZ^{*}\rho}{k}\exp\left(\frac{-E_a}{kT}\right). \quad (2)$$

Taking the logarithm of both sides of Eq. (2),

$$\ln\frac{vT}{j}=-\left(\frac{E_a}{kT}\right)+\ln\frac{D_0eZ^{*}\rho}{k}. \quad (3)$$

Therefore, by measuring the solder drift velocity as a function of reciprocal temperature, the activation energy E_a and the product of diffusivity and effective charge number, DZ^*, can be obtained.

Figure 8 shows the plot of $\ln(vT/j)$ as a function of the reciprocal temperature. The activation energy (E_a) can be determined from the slope of the fitted line, and its value is 0.41 eV in the temperature range of 80–120 °C. However, the temperature in the solder needs to be calibrated due to the Joule heating effect, as shown in Fig. 4. The real temperatures in the solder were higher than the ambient ones, and the activation energy was calculated to be 0.45 eV using the real temperatures.

In addition, the product of diffusion diffusivity and effective charge number, DZ^*, can be calculated from Eq. (3). Table I summarizes the product of the diffusivity and effective charge number, DZ^*, and its average values are -1.8×10^{-10} cm^2/s at 80 °C, -5.0×10^{-10} cm^2/s at 100 °C, and -7.2×10^{-10} cm^2/s at 120 °C. In order to estimate the value of Z^*, the diffusivity data for pure Sn were adopted.[17] The

[This article is copyrighted as indicated in the article. Reuse of AIP content is subject to the terms at: http://scitation.aip.org/termsconditions. Downloaded to] IP: 140.113.38.11 On: Thu, 01 May 2014 02:55:08

TABLE I. The product of diffusivity and effective charge number (DZ^*) for various stressing conditions.

Temperaure (°C)	Currnt density (A/cm^2)	DZ^* (cm^2/s)
80	1.0×10^5	-2.26×10^{-10}
80	8.4×10^4	-1.72×10^{-10}
80	7.1×10^4	-1.61×10^{-10}
		Ave.: -1.86×10^{-10}
100	9.0×10^4	-6.88×10^{-10}
100	6.2×10^4	-5.35×10^{-10}
100	4.4×10^4	-2.80×10^{-10}
		Ave.: -5.01×10^{-10}
120	7.5×10^4	-1.03×10^{-9}
120	5.7×10^4	-1.03×10^{-9}
120	4.0×10^4	-8.12×10^{-10}
120	2.0×10^4	-3.37×10^{-10}
		Ave.: -7.26×10^{-10}

average values of Z^* were −27 at 80 °C, −33 at 100 °C, and −23 at 120 °C, which are reasonable for solder materials.

IV. DISCUSSION

A. Threshold current density of $SnAg_{3.8}Cu_{0.7}$ solder stripes

To verify if these extrapolated values of threshold current density are correct or not, some specimens were stressed at current densities below the threshold current density. Specimens were stressed at the current density of 3.5×10^4 A/cm^2 at 80 °C, 2.6×10^4 A/cm^2 at 100 °C, and 1×10^4 A/cm^2 at 100 °C for 72 h, and no detectable volume change was found.

Various stressing conditions have been investigated to study the electromigration behavior of SnAgCu bumps, and a large variety of conditions was reported to have caused damage in the bumps. Wu *et al.* conducted a MTTF experiment for $SnAg_{4.0}Cu_{0.5}$ bumps with thin-film underbump metallization (UBM) of Al/Ni(V)/Cu, and found that the MTTF was 1454 h for the bumps stressed by 5.0×10^3 A/cm^2 at 153 °C.[11] In addition, Choi *et al.* reported that the eutectic SnAgCu bumps with Al/Ni(V)/Cu UBM failed after the current stressing at 2.25×10^4 A/cm^2 at 140 °C for 132 h.[7] However, Lin *et al.* investigated the current carrying capability of eutectic SnAgCu bumps with 6-μm Ni underbump metallization, and found that there was no obvious electromigration damage in the bumps after the stressing by 2.55×10^4 A/cm^2 at 150 °C for 2338 h.[12]

The above discrepancies may be due to the serious current crowding in the line-to-bump configuration of flip-chip solder joints and also the Joule heating effect in the solder joints. Our previous simulation study on current-density distribution showed that the joints with thin-film Al/Ni(V)/Cu UBM had more serious current crowding effect inside the solder bumps than that in the joints with thick UBM.[18] The current crowding ratio may be as high as 23 inside the solder for the joints with thin-film Al/Ni(V)/Cu UBM, which means that the maximum current density near the solder close to the entrance point of Al trace is 23 times higher than the average value. Thus the maximum current density in these solder bumps may exceed 1.0×10^5 A/cm^2. However, the current crowding ratio for the bumps with 6-μm electroless Ni UBM is about 11, leading to a higher current carrying capability by these bumps. On the other hand, Joule heating may increase the temperature of the solder bump, and the amount of temperature increase depends on the joint geometry, materials, and applied current. Choi *et al.* found that the temperature increase due to Joule heating was between 38 and 52 °C.[7] Therefore, the real stressing temperature was higher than 178 °C for their bumps. Based on the above discussion, the threshold current density in the present work seems to be reasonable.

B. Activation energy of eutectic $SnAg_{3.8}Cu_{0.7}$ solder stripes

The activation energy we measured by edge displacement technique was 0.45 eV, which was lower than the published value. Choi *et al.* measured the MTTF of eutectic SnAgCu solder joints, and they estimated the activation energy to be 0.8 eV by using Black's equation.[7] It is speculated that the difference may be attributed to the smaller grain size of the solder in Blech specimens than in flip-chip solder joints. As shown in Fig. 3(b), the grain size of the solder was only about 1 μm, which is smaller than that in the solder bumps. In addition, the stressing temperatures in this study ranged from 70% to 77% of the absolute melting point of the eutectic SnAgCu solder. Therefore, the activation energy presented in this study is a combination of grain boundary and lattice diffusion. As a result, the contribution of grain-boundary diffusion may be larger in our sample, resulting in a decrease in the activation energy for the solder film. The effect of grain-boundary diffusion may have also affected the value of the estimate effect charge number which is smaller than what is expected in a bulk Sn sample.

C. Electromigration of Cu_6Sn_5 intermetallic compounds

Theoretically, a 1.36-μm-thick Cu_6Sn_5 layer formed when the 0.4-μm Cu was entirely consumed during the reflow process. Our cross-sectional TEM results show that the average thickness of Cu_6Sn_5 was 1.42 μm, which almost matches the theoretical value. Therefore, the Cu layer was almost consumed completely. In addition, the composition of the solder may not change much, since we applied a large amount of solder paste on the UBM during the reflow process, and then the excess solder was polished away, as described in the Experiment section. Consequently, the composition of the SnAgCu is expected to remain close to the eutectic composition.

The Cu_6Sn_5 IMC exhibited a better electromigration resistance than the $SnAg_{3.8}Cu_{0.7}$ solder, since the IMC remained intact after electromigration test for most of the specimens, as shown in Fig. 5(b). However, for some specimens stressed at more stringent conditions, the IMC on the cathode end was also found to migrate away after the depletion of the solder. Figures 9(a) and 9(b) demonstrate the microstructure evolution in the $SnAg_{3.8}Cu_{0.7}$ solder stripe be-

[This article is copyrighted as indicated in the article. Reuse of AIP content is subject to the terms at: http://scitation.aip.org/termsconditions. Downloaded to] IP: 140.113.38.11 On: Thu, 01 May 2014 02:55:08

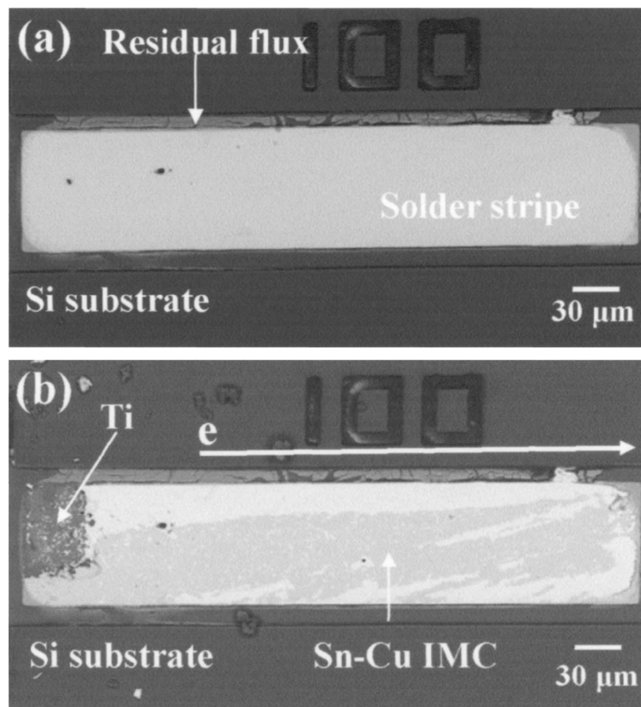

FIG. 9. (a) Plan-view BSE SEM image of a $SnAg_{3.8}Cu_{0.7}$ solder stripe before current stressing. (b) Plan-view BSE SEM image of the stripe after stressing at 120 °C for 30 h. The Cu_6Sn_5 IMC layer was also migrated after the current stressing.

fore and after the stressing by 1.2×10^5-A/cm^2 current density for 30 h at 120 °C, respectively. Both the $SnAg_{3.8}Cu_{0.7}$ solder and Cu_6Sn_5 IMC were migrated by electron flow on the cathode side. In the meantime, Sn–Cu compounds were observed in the stripe after the current stressing. When the upper solder was depleted by the electron flow, the current density flowing in the remaining Cu_6Sn_5 IMC became higher. This was because the resistivity of the IMC (17.5 $\mu\Omega$ cm) was lower than that of the Ti layer (43.1 $\mu\Omega$ cm), and the thickness of the IMC was thicker than that of the Ti layer. For the above stressing condition, it was estimated that the current density in the IMC layer after the complete depletion of the solder was about 1×10^5 A/cm^2. Therefore, the Cu_6Sn_5 IMC may migrate under such high current density. However, the electromigration study for the IMC needs to be investigated independently in order to measure the threshold current density.

V. CONCLUSIONS

The $SnAg_{3.8}Cu_{0.7}$ Blech test specimens have been successfully fabricated to investigate the electromigration behavior under various current densities in the temperature range of 80–120 °C. We used AFM to measure the drift velocity and analyzed the electromigration behavior of the Pb-free solder. The threshold current densities were measured to be 4.3×10^4 A/cm^2 at 80 °C, 3.2×10^4 A/cm^2 at 100 °C, and 1.4×10^4 A/cm^2 at 120 °C. The measured activation energy was 0.45 eV for the temperature ranges from 80 to 120 °C. The measured product of diffusivity and effective charge number, DZ^*, was -1.8×10^{-10} cm^2/s at 80 °C, -5.0×10^{-10} cm^2/s at 100 °C, and -7.2×10^{-10} cm^2/s at 120 °C.

ACKNOWLEDGMENT

The authors would like to acknowledge the financial support of the National Science Council of Taiwan through Grant No. NSC92-2216-E009-008.

[1] J. H. Lau and S.-W. R. Lee, *Chip Scale Package* (McGraw-Hill, New York, 1999), p. 3.
[2] S. Brandenburg and S. Yeh, *Proceedings of Surface Mount International Conference and Exhibition*, San Jose, CA, 23–27 August 1998 (Integrated Electronics Engineering Center, New York, 1998), p. 337.
[3] K. N. Tu, J. Appl. Phys. **94**, 5451 (2003).
[4] K. Zeng and K. N. Tu, Mater. Sci. Eng., R. **38**, 55 (2002).
[5] D. Suraski and K. Seelig, IEEE Trans. Electron. Packag. Manuf. **24**, 244 (2001).
[6] see website "www.nemi.org/PbFreePUBLIC"
[7] W. J. Choi, E. C. C. Yeh, and K. N. Tu, J. Appl. Phys. **94**, 5665 (2003).
[8] T. Y. Lee, K. N. Tu, and D. R. Frear, J. Appl. Phys. **90**, 4502 (2001).
[9] S. Y. Jang, J. Wolf, W. S. Kwon, and K. W. Paik, *Proceedings of the 52nd Electronic Components and Technology Conference*, IEEE Components, Packaging, and Manufacturing Technology Society, San Diego, CA, 2002 (IEEE, New York, 2002), p. 1213.
[10] Y. C. Hsu, T. L. Shao, C. J. Yang, and C. Chen, J. Electron. Mater. **32**, 1222 (2003).
[11] J. D. Wu, C. W. Lee, P. J. Zheng, J. C. B. Lee, and S. Li, *Proceedings of the 54th Electronic Components and Technology Conference*, IEEE Components, Packaging, and Manufacturing Technology Society, Las Vegas, NV, 2004 (IEEE, New York, 2004), p. 961.
[12] J. K. Lin, J. W. Jang, and J. White, *Proceedings of the 53rd Electronic Components and Technology Conference*, IEEE Components, Packaging, and Manufacturing Technology Society, New Orleans, LA, 2003 (IEEE, New York, 2003), p. 816.
[13] I. A. Blech, J. Appl. Phys. **47**, 1203 (1976).
[14] I. A. Blech, Acta Mater. **46**, 3717 (1998).
[15] T. L. Shao, S. H. Chiu, C. Chen, D. J. Yao, and C. Y. Hsu, J. Electron. Mater. **33**, 1350 (2004).
[16] H. B. Huntigton and A. R. Grone, J. Phys. Chem. Solids **20**, 76 (1961).
[17] P. H. Sun and M. Ohring, J. Appl. Phys. **47**, 478 (1976).
[18] T. L. Shao, S. W. Liang, T. C. Lin, and C. Chen, J. Appl. Phys. (to be published).

[This article is copyrighted as indicated in the article. Reuse of AIP content is subject to the terms at: http://scitation.aip.org/termsconditions. Downloaded to] IP: 140.113.38.11 On: Thu, 01 May 2014 02:55:08